https://doi.org/10.5194/egusphere-2023-2595
Preprint. Discussion started: 9 November 2023

Distribution and source attribution of alkalinity in the Dutch Wadden Sea

Mona Norbisrath[1], Justus E. E. van Beusekom[1], & Helmuth Thomas[1,2]

[1]Institute of Carbon Cycles, Helmholtz-Zentrum Hereon, Geesthacht, 21502, Germany

[2]Institute for Chemistry and Biology of the Marine Environment (ICBM), Carl von Ossietzky University Oldenburg, Oldenburg, 26129, Germany

Correspondence to: Mona Norbisrath (mona.norbisrath@gmail.com)

Abstract

As the major global CO_2 sink, the oceanic buffering capacity total alkalinity (TA) is of growing scientific interest. TA is mainly generated by weathering, and further by various anaerobic metabolic processes. The Wadden Sea, located in the southern North Sea is thought to be a source of TA for the carbonate system of the North Sea, but quantifications are scarce. Here, we observed TA, dissolved inorganic carbon (DIC), and nutrients in the Dutch Wadden Sea in May 2019. We sampled transect surface waters to detect spatial distributions and compared it with earlier data. A tidal cycle was sampled to further shed light on TA generation and potential TA sources. We identified the Wadden Sea as a source of TA with an average TA generation of 7.6 µmol kg^{-1} h^{-1} during ebb tide in the Ameland Inlet. TA was generated in the sediments and washed out with off running water. A combination of anaerobic processes and $CaCO_3$ dissolution were potential sources of TA in the sediments. We assume that seasonality and the associated nitrate availability in particular influence TA generation by denitrification, which we assume is low in spring and summer.

1 Introduction

As the regulator of the ocean carbon dioxide (CO_2) sink, total alkalinity (TA) is of increasing scientific interest and investigated worldwide in the Anthropocene (Abril and Frankignoulle, 2001;Bozec et al., 2005;Chen and Wang, 1999;Dickson, 1981;Middelburg et al., 2020;Norbisrath et al., 2022;2023;Renforth and Henderson, 2017;Thomas et al., 2004;2009;Sabine et al., 2004). The Anthropocene describes the current era of our planet, when environmental changes, driven by humans, have become identifiable in geological records (Zalasiewicz et al., 2010;Crutzen, 2002). Coastal regions, which are the direct interface between most, if not all, compartments of the Earth system (i.e., terrestrial, aquatic, oceanic) and human societies, appear particularly vulnerable to environmental and climate change (Glavovic et al., 2015). This holds true for the Wadden Sea, the shallow, coastal sea along an approximately 500 km coastline of the Netherlands, Germany, and Denmark, in the southern North Sea, which is declared as an UNESCO world natural heritage site since 2009. Most part of it is located between the protecting barrier Islands and the Mainland, which makes it a unique and the world's largest uninterrupted stretch of tidal flats with multiple tidal inlets (Fig. 1). Due to the topography, the Wadden Sea is a highly dynamic ecosystem with influences

https://doi.org/10.5194/egusphere-2023-2595
Preprint. Discussion started: 9 November 2023

from the mainland and the North Sea (Hoppema, 1993;Postma, 1954;Raaphorst and Veer, 1990). Driving forces of the dynamics in the Wadden Sea are nutrient and organic matter (OM) imports by rivers, high suspended particulate matter (SPM) imports by the North Sea (Van Beusekom et al., 2012;Postma, 1954), and oceanic driven wind, waves, and tidal currents, as well as the counterclockwise circulation of the North Sea (Elias et al., 2012). Large tidal amplitude and currents in conjunction with shallow water depths allow for vertical water column mixing and an exchange between the benthic and pelagic realms. The high tidal currents also impact the biogeochemistry of the North Sea (Postma, 1954), as they cause a strong exchange of water masses.

The North Sea and its carbon storage capacity is an important atmospheric CO_2 sink by exporting and storing the absorbed CO_2 in the deep layers of the Atlantic Ocean (Schwichtenberg et al., 2020;Thomas et al., 2004;2009;Burt et al., 2016;Borges et al., 2005;Hu and Cai, 2011;Brenner et al., 2016).

Next to chemical rock weathering (Suchet and Probst, 1993;Meybeck, 1987;Berner et al., 1983), TA, usually consisting of bicarbonate and carbonate, is also generated in various stoichiometries by calcium carbonate ($CaCO_3$) dissolution and anaerobic metabolic processes, such as denitrification, which is the reduction process of nitrate to dinitrogen gas in the nitrogen cycle (Hu and Cai, 2011;Wolf-Gladrow et al., 2007;Chen and Wang, 1999;Brewer and Goldman, 1976).

Understanding of TA sources have recently become increasingly important due to increasing anthropogenic CO_2 emissions, and the resulting demand for ocean based net-negative CO_2 emissions (e.g., Keith et al., 2006;Matthews and Caldeira, 2008;Zhang et al., 2022).

In previous studies, the Wadden Sea was estimated as a TA source of the North Sea with a loading between 39 Gmol yr^{-1} (Schwichtenberg et al., 2020) and 73 Gmol yr^{-1} (Thomas et al., 2009). Both studies suggested the entire Wadden Sea as one of the most important TA sources of the carbon storage capacity of the North Sea. Burt et al. (2016) highlighted the importance of coastal TA production for regulating the buffer system in the North Sea, whereby they suggest denitrification as the major TA source. Due to the strong connection between the North Sea and the Wadden Sea, a better understanding of TA generation in the latter one is required. Here, we focus on the Dutch Wadden Sea that has been well-studied during the past decades (Hoppema, 1990, 1991, 1993;De Jonge et al., 1993;Elias et al., 2012;Ridderinkhof et al., 1990;Postma, 1954;Van Beusekom et al., 2019;Schwichtenberg et al., 2017). In particular Hoppema (1990);(1993) observed the spatial and temporal variability of TA, which we compare with our observed transect data to detect potential differences over the last 30 years. In addition, we further shed light on potential TA sources in the Dutch Wadden Sea.

2 Methods

2.1 Study site and sampling

This study is based on samples collected on a research cruise (LP20190515) in the Dutch Wadden Sea (Frisian Islands) on RV *Ludwig Prandtl* in May 2019 (Fig. 1). We collected water samples in the Wadden Sea starting at Harlingen, through the Vlie Inlet around the islands Vlieland and Terschelling, through the Ameland Inlet to Ameland Island, from there on via the Frisian

https://doi.org/10.5194/egusphere-2023-2595
Preprint. Discussion started: 9 November 2023

Inlet to Lauwersoog, and around Schiermonnikoog Island via the Ems-Dollard Inlet to Emden. Nearly half-hourly, we continuously collected discrete surface (1.2 m depth) water samples with a bypass from the onboard flow-through FerryBox system (Petersen et al., 2011), which provided essential physical parameters such as salinity and temperature. In addition, we sampled a tidal cycle from high tide to low tide and from low tide to high tide on each of two days as an anchor station in the waterway at the western side of Ameland in the Ameland Inlet.

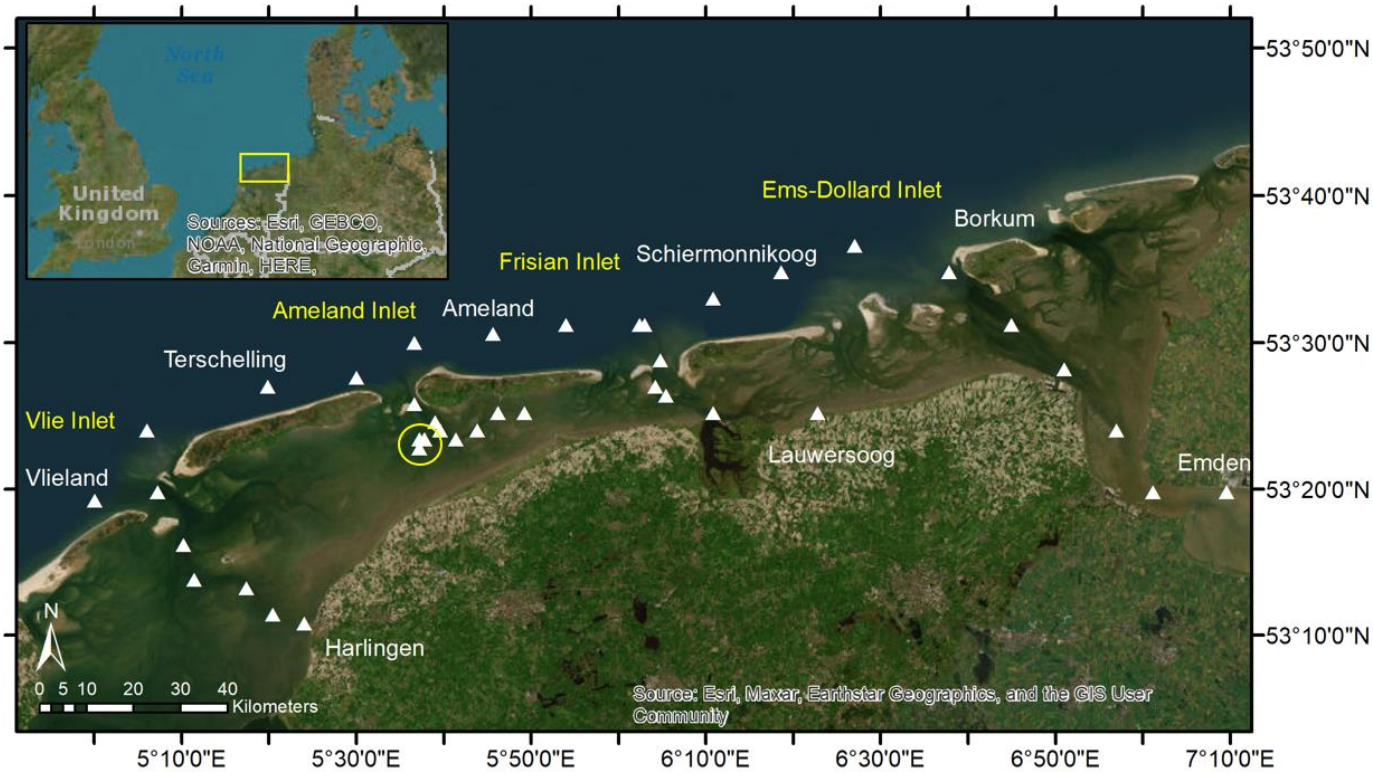

Figure 1 Sampling site in the Dutch Wadden Sea. The sampling stations around the Frisian Islands in May 2019 are visualized with the white triangles. The yellow circle highlights the anchor stations for the tidal cycle sampling in the Ameland Inlet on two days. During the sampling day from low tide to high tide, we had two samples that we took slightly more western due to drifting. The island and city names are shown in white, the inlets in yellow. The tidal flats and sedimentary structures are well visible between the barrier islands and the mainland.

2.2 Sampling and analysis

2.2.1 Carbon species

For carbon measurements we sampled water with overflow into 300 mL BOD (biological oxygen demand) bottles and preserved them with 300 µL saturated mercury chloride ($HgCl_2$) to stop biological activity. Each BOD bottle was filled without

https://doi.org/10.5194/egusphere-2023-2595
Preprint. Discussion started: 9 November 2023

air bubbles and closed by using a ground-glass stopper coated in Apiezon® type M grease and a plastic cap. The samples were stored in a cool dark environment until measurements in the lab.

The parallel analyses of TA and DIC were carried out by using the VINDTA 3C (Versatile INstrument for the Determination of Total dissolved inorganic carbon and Alkalinity, MARIANDA - marine analytics and data), which measures TA by potentiometric titration and DIC by coulometric titration with a measurement precision < 2 µmol kg^{-1}. (Shadwick et al., 2011). To ensure a consistent calibration of both measurements, we used Certified Reference Material (CRM batch # 187) provided by Andrew G. Dickson (Scripps Institution of Oceanography).

The calcite saturation state (Ω) and the pH were computed with the CO_2SYS program (Lewis and Wallace, 1998), using the measured parameters TA, DIC, salinity, temperature, silicate and phosphate as input variables, together with the dissociation constants from Mehrbach et al. (1973), as refit by Dickson and Millero (1987).

2.2.2 Nutrients

Water for nutrient samples was filtered through pre-combusted (4 h, 450 °C) GF/F filters to store them afterwards frozen in three 15 mL Falcon tubes for triplicate measurements in the lab.

We measured the nutrients with a continuous flow automated nutrient analyzer (AA3, SEAL Analytical) and a standard colorimetric technique (Hansen and Koroleff, 2007) for nitrate (NO_3^-), nitrite (NO_2^-), phosphate (PO_4^{3-}), and silicate (Si), and a fluorometric method (Kérouel and Aminot, 1997) for ammonium (NH_4^+) (Grasshoff et al., 2009).

In order to determine the total carbon (C), organic carbon (C_{org}) and nitrogen (N) concentrations in SPM and associated C_{org}:N ratios, we used pre-combusted (4 h, 450 °C) GF/F filters, which we dried after sampling at 50 °C to remove all humidity and stored frozen until measurement. For the C_{org} determination, filters were acidified with 1N HCl and dried overnight to remove all inorganic carbon content. Filters were measured with a CHN-elemental analyzer (Eurovector EA 3000, HEKAtech GmbH) in the Institute of Geology, University Hamburg, and calibrated against a certified acetanilide standard (IVA Analysentechnik, Germany). The standard deviations were 0.05 % for carbon and 0.005 % for nitrogen.

3 Results

3.1 Spatial parameter distribution

In order to investigate the spatial distribution of total alkalinity (TA) in the Dutch Wadden Sea and compare its general status with the past, we observed the spatial distribution of TA and related parameters from the coastal mainland towards the open ocean as surface water transect.

The temperatures varied between 12 and 16 °C with higher temperatures towards the coastal mainland (Fig. 2a). Salinity was relatively stable with only minor differences varying from 28 to 33 (Fig. 2b). Lower salinities were only observed in the four sampling stations in the Ems Estuary with the minimum value of 20.25 at the most upstream station.

https://doi.org/10.5194/egusphere-2023-2595
Preprint. Discussion started: 9 November 2023

Spatial transect TA concentrations ranged from 2332 µmol kg^{-1} to 2517 µmol kg^{-1}. We observed lower concentrations on the oceanic, i.e., North Sea side of the Frisian Islands with somewhat higher concentrations around Ameland (Fig. 2c). In contrast to the oceanic side, the concentrations were higher with values > 2380 µmol TA kg^{-1} in the Wadden Sea. Only in the Ems Estuary, the concentrations were even higher, with values up to 2517 µmol TA kg^{-1} at the most upstream station. We saw higher TA values in the Wadden Sea than in the open ocean, supporting the assumption of TA being generated in this tidal flat area. We also observed highest TA concentrations at the coastal mainland that decreased towards the North Sea.

In silicate (Si), we observed a similar pattern as in TA, with higher concentrations in the Wadden Sea and lower ones towards the ocean (Fig. 2d). Highest concentrations were observed at the coastal mainland and in the Ems Estuary. Silicate concentrations were between 0.26 and 56.32 µmol L^{-1}.

The calcite saturation state (Ω) was supersaturated in the entire observed study site (Fig. 2e). We observed values from 2.32 to 4.65. Highest values were observed at the oceanic side of the barrier islands in the North Sea. Lowest values were observed near Harlingen and in the Ems Estuary.

Similar to the calcite saturation state (Ω), we observed higher pH values in the North Sea and lower values in the Wadden Sea and near the coastal mainland (Fig. 2f). The pH values ranged from 7.86 to 8.19. Lowest values were observed near Harlingen and in the Ems Estuary.

The nitrate (NO_3^-) concentrations were similar in a low range (< 3 µmol NO_3^- L^{-1}) in the entire transect, with higher concentrations (< 6 µmol NO_3^- L^{-1}) at only a few stations close to land, and maximum concentrations (< 38 µmol NO_3^- L^{-1}) in the Ems Estuary (Fig. 2g).

Concentrations of DIC ranged from 2097 µmol kg^{-1} to 2430 µmol kg^{-1} (Fig. 2h). DIC values were similar to TA values, with higher concentrations near the coastal mainland and in the Ems Estuary, and decreasing concentrations toward the North Sea, where we observed lowest DIC concentrations.

https://doi.org/10.5194/egusphere-2023-2595
Preprint. Discussion started: 9 November 2023

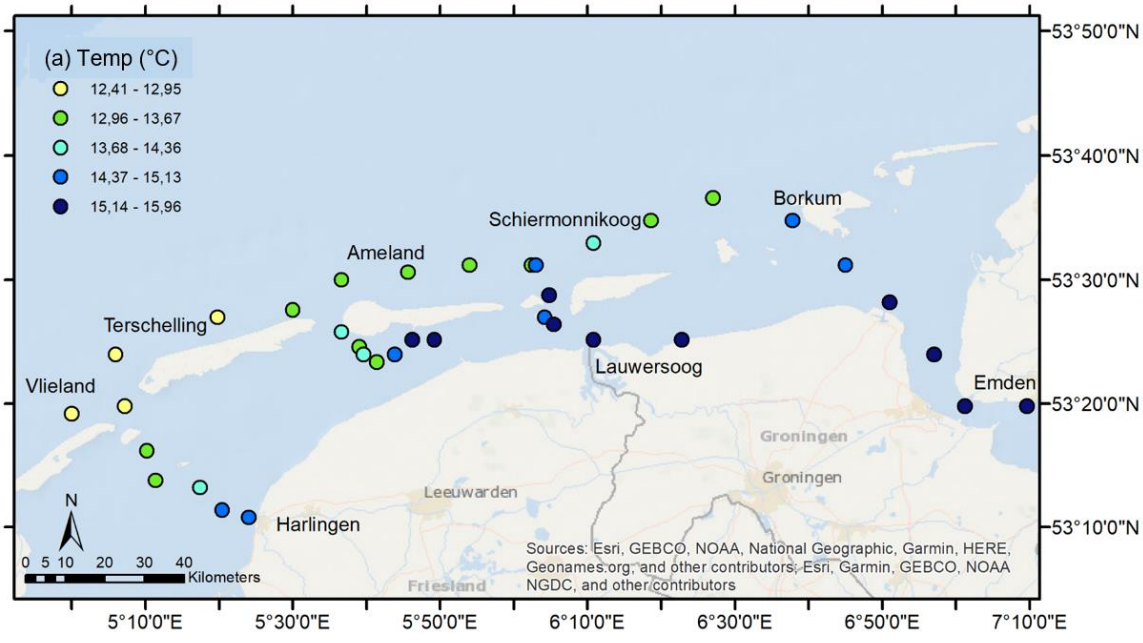

129

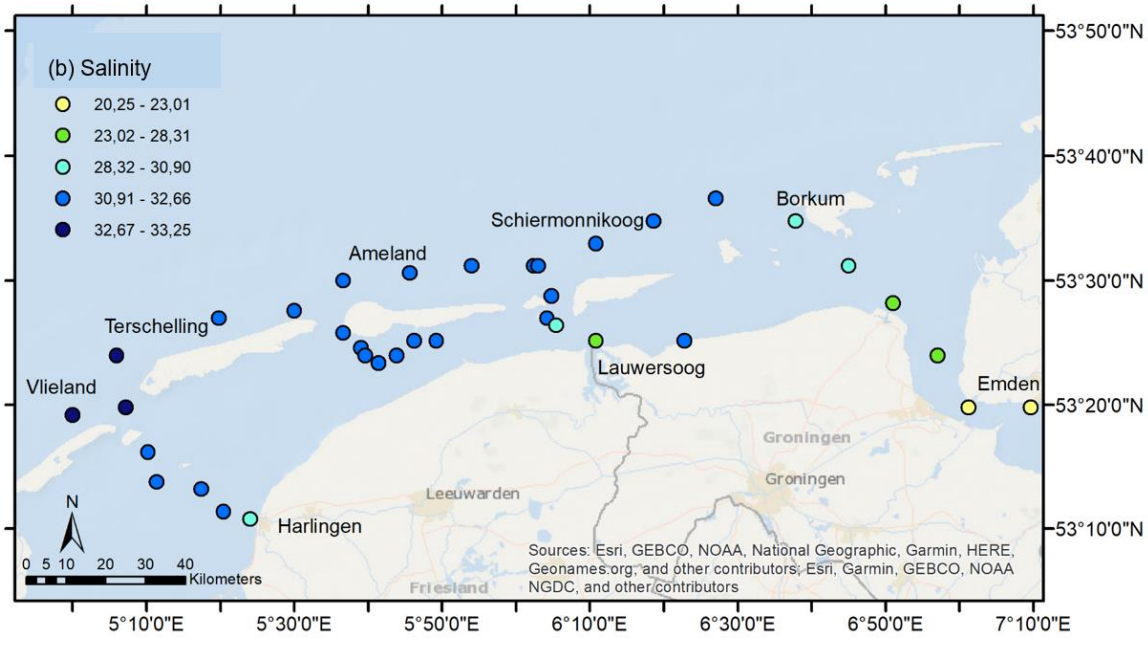

130

https://doi.org/10.5194/egusphere-2023-2595
Preprint. Discussion started: 9 November 2023

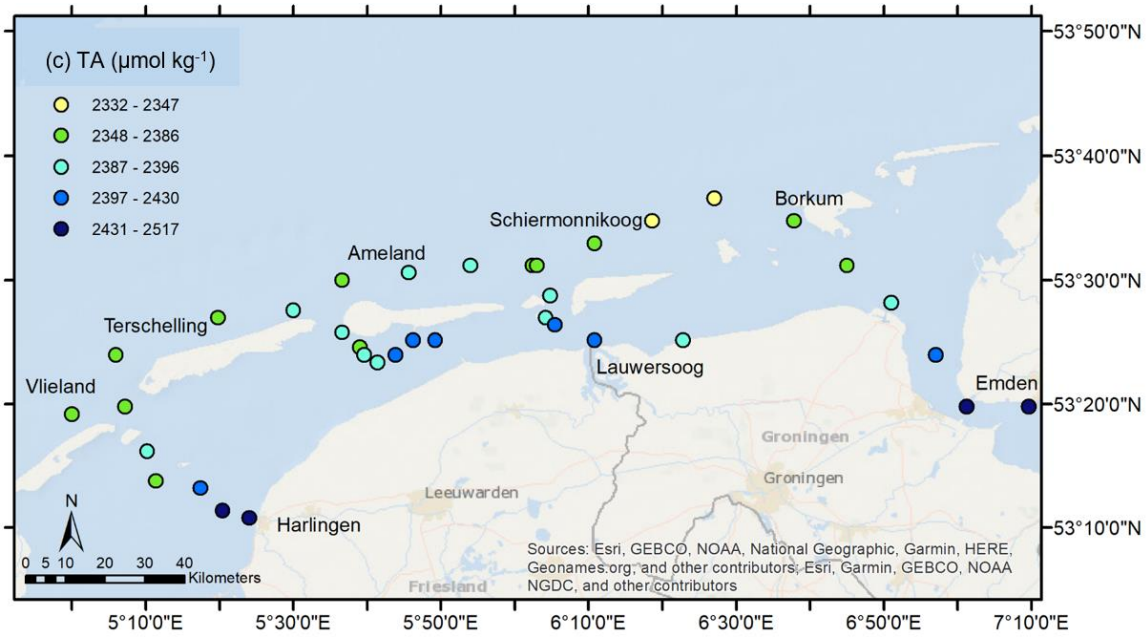

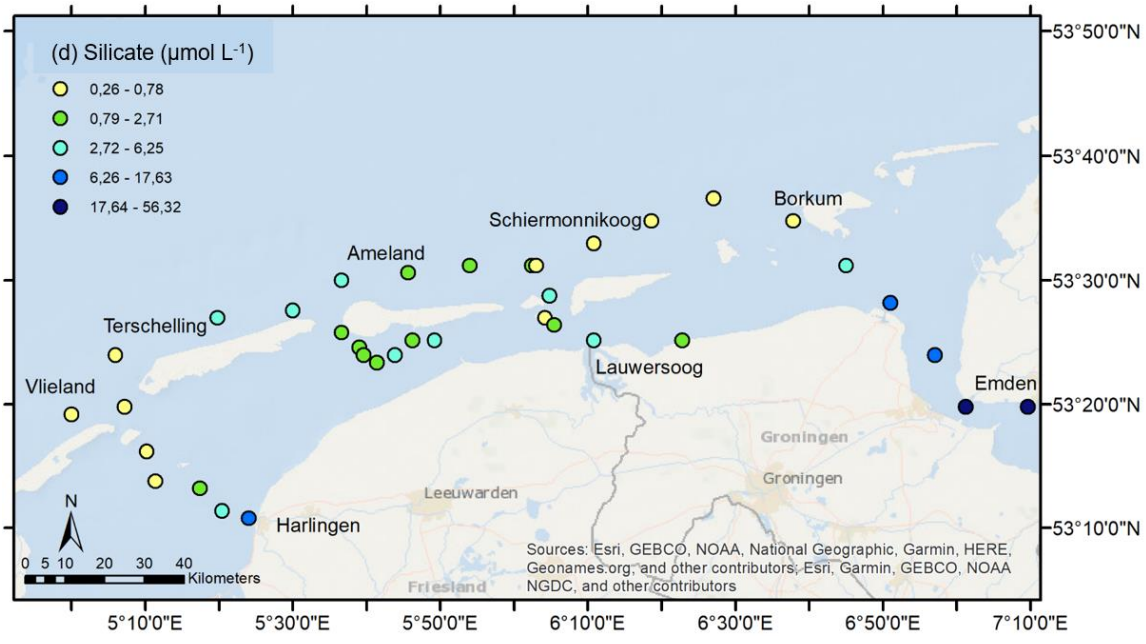

https://doi.org/10.5194/egusphere-2023-2595
Preprint. Discussion started: 9 November 2023

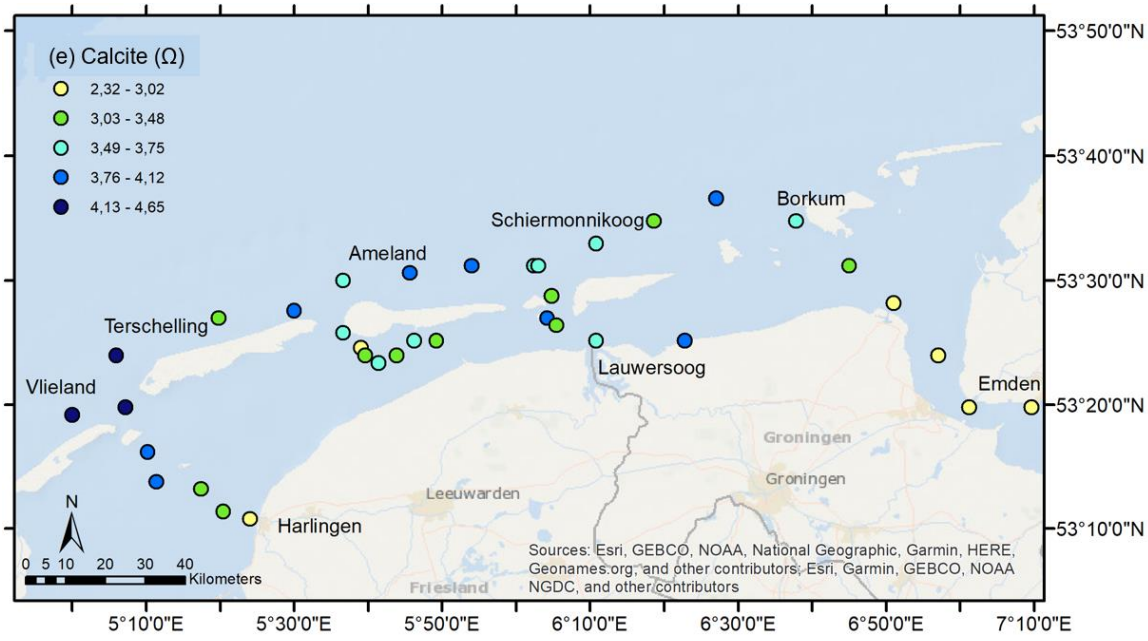

133

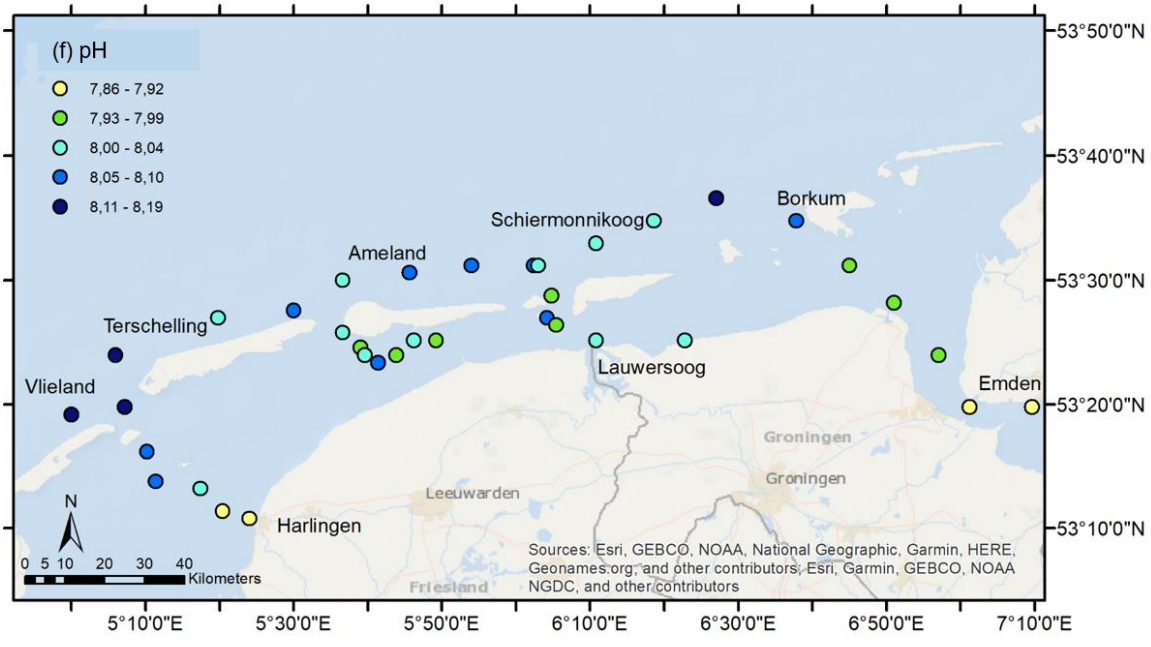

134

https://doi.org/10.5194/egusphere-2023-2595
Preprint. Discussion started: 9 November 2023

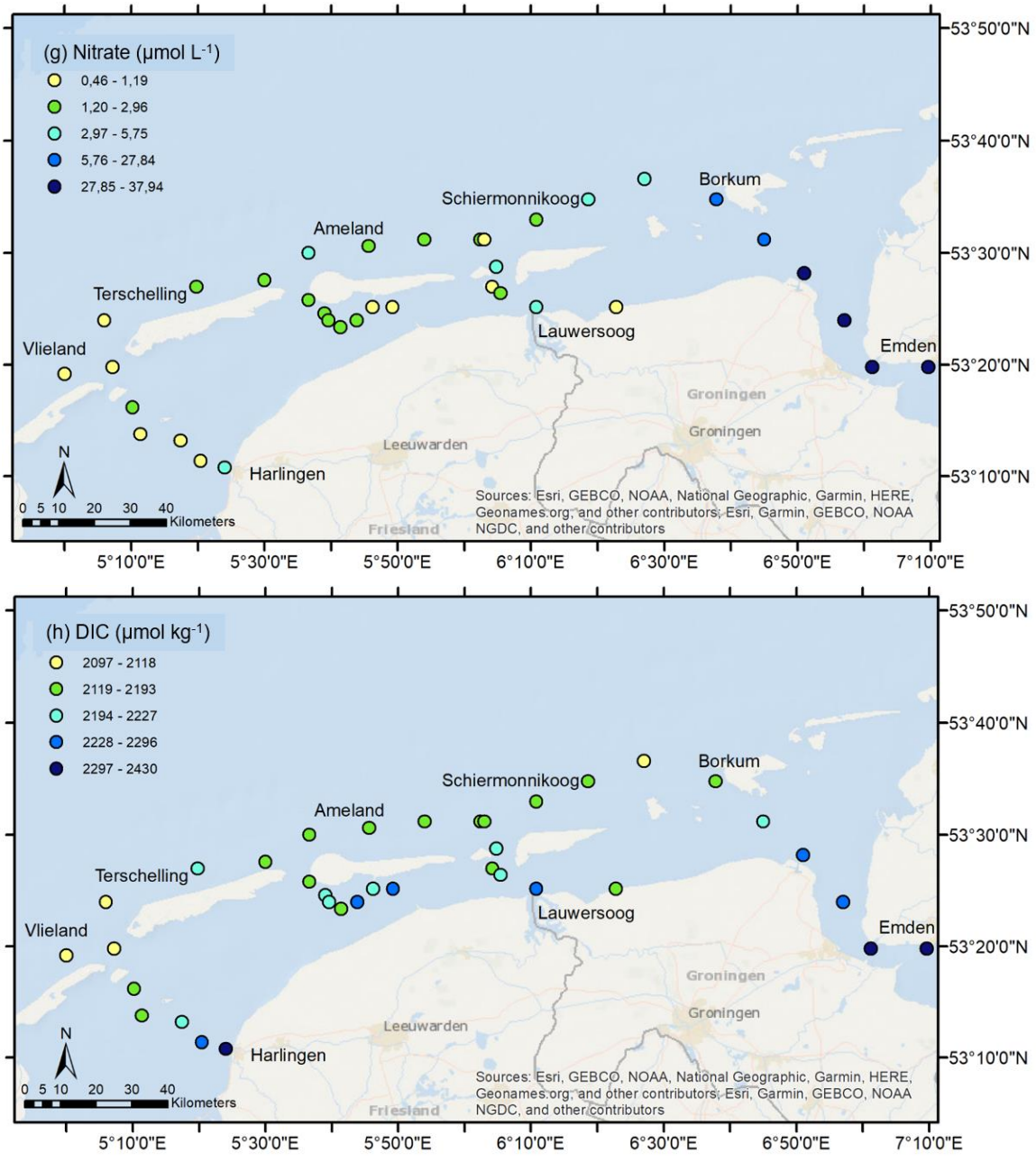

Figure 2 Spatial distribution of various parameters. Latitudinal and longitudinal distribution of a) temperature (°C), b) salinity, c) total alkalinity (TA; µmol kg^{-1}), d) silicate (Si; µmol L^{-1}), e) calcite saturation state (Ω), f) pH, g) nitrate (NO_3^-; µmol L^{-1}), and h) dissolved inorganic carbon (DIC; µmol kg^{-1}) from surface water samples in May 2019.

The strong impact from the Ems Estuary is visible in all parameters with higher values in the outer estuary and its adjacent zones, or with lower values in case of pH and the calcite saturation state. Furthermore, we observed higher values around

https://doi.org/10.5194/egusphere-2023-2595
Preprint. Discussion started: 9 November 2023

Ameland Island than in the western part on our transect starting from Harlingen towards the Vlie Inlet. In particular at the oceanic side from the Vlie Inlet, the impact of the North Sea is visible through lower temperatures and higher salinities. The North Sea impact is also visible in the mixing between TA and salinity (Fig. 3). We only observed a relatively linear mixing behavior in the transect through the Ems-Dollard Inlet and Vlie Inlet (Fig. 3). There, we observed decreasing TA concentrations with increasing salinities from the mainland towards the ocean (Fig. 3). Therefore, we identified the Dutch Wadden Sea as being a source of TA. We detected higher TA concentrations than the TA concentration computed for the salinity end-member in the Ems-Dollard Inlet in the oceanic, i.e., North Sea side of Ameland (Ameland NS), in the Wadden Sea side of Amland (Ameland WS), and in the Vlie Inlet, indicating towards additional TA sources. The Ameland NS and Ameland WS data clearly indicated non-conservative behavior with increasing TA concentrations and constant salinities.

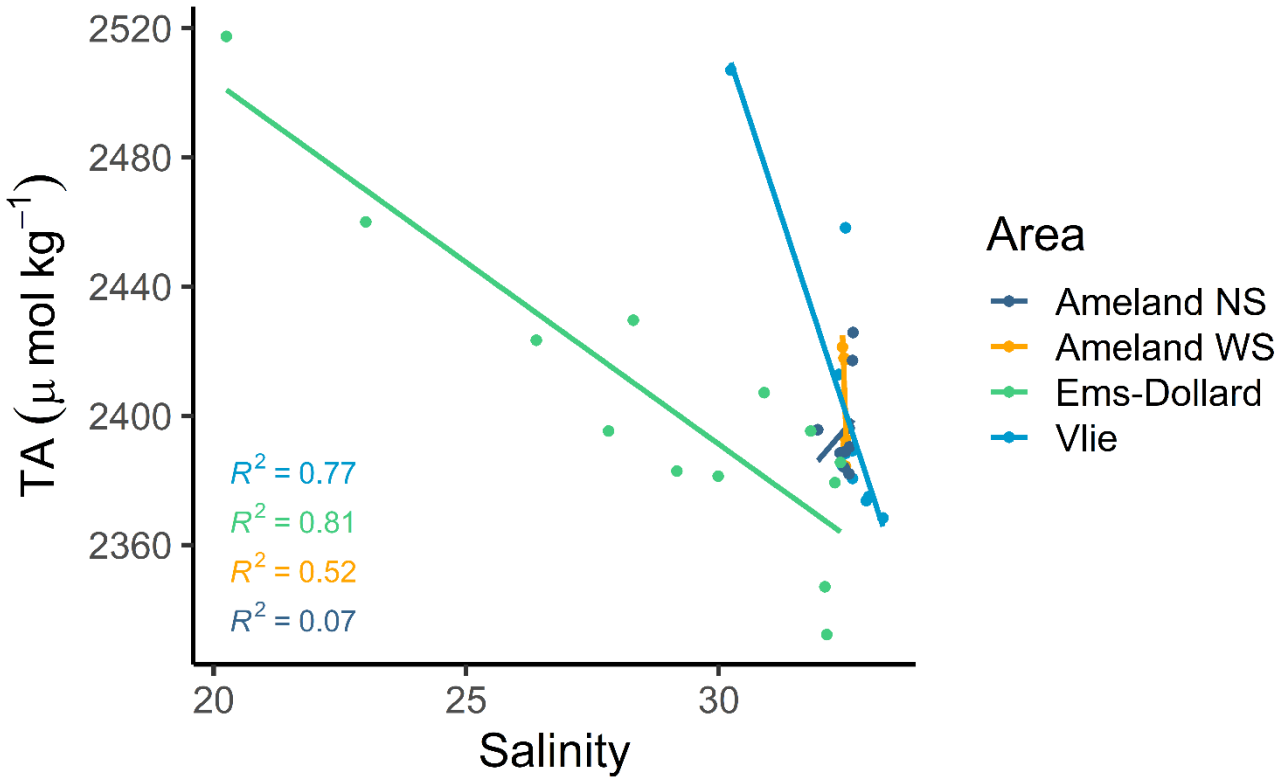

Figure 3 Total alkalinity - salinity mixing. Mixing between total alkalinity (TA) and salinity in the oceanic side of Ameland and the Frisian Inlet (Ameland NS), in the Wadden Sea site of Ameland (Ameland WS), around Schiermonnikoog and in the Ems-Dollard Inlet, and in the Vlie Inlet.

https://doi.org/10.5194/egusphere-2023-2595
Preprint. Discussion started: 9 November 2023

3.2 Tidal cycle

In order to estimate TA generation in the Dutch Wadden Sea, to shed light on potential TA sources, and to estimate the potential TA amount that is exported to the North Sea, we observed a tidal cycle at an anchor station in the Ameland Inlet on two days with the observation of flood tide and ebb tide, respectively. Here, our focus is on ebb tide data that we used to identify pattern in the various parameters in off running water (Table 1).

During ebb tide, TA ranged from high tide with 2387 µmol TA kg^{-1} to low tide with 2438 µmol TA kg^{-1} (Fig. 4a). We identified an increase of 51.6 µmol TA kg^{-1} (ΔTA) over a duration of 6.8 h during ebb tide, resulting in a TA increase of 7.6 µmol TA kg^{-1} h^{-1} at the sampling location.

DIC concentrations were similar to TA with minimum values at high tide (2172 µmol DIC kg^{-1}) and highest values (2273 µmol DIC kg^{-1}) at low tide. During ebb tide, we observed an increase of 101.3 µmol DIC kg^{-1} (ΔDIC) resulting in a DIC increase of 14.9 µmol DIC kg^{-1} h^{-1} (Fig. 4b). DIC increased almost twice as much as TA.

In silicate, we detected a similar pattern with low values (1.8 µmol Si L^{-1}) at high tide and increasing concentrations during ebb tide to a maximum of 11.2 µmol L^{-1}. The silicate increase (ΔSi) of 9.4 µmol Si L^{-1} resulted in a silicate increase of 1.4 µmol L^{-1} h^{-1} during ebb tide (Fig. 4c).

The salinity observations allow us to exclude conservative mixing for dilution, since the salinity was constant between 32.50 and 32.52 (Fig. 4d). We observed values in the range of saline waters similar to water of the North Sea.

The calcite saturation state (Ω) had a maximum value (3.8) at high tide and decreased to 3.1 during ebb tide (Fig. 4e). The maximum at high tide indicated the influence of the North Sea that reduced with off running water.

Similar to omega, the pH had maximum values (8.07) at high tide and decreased to a minimum of 7.93 during ebb tide (Fig. 4f). We observed decreasing pH with off running water.

Nitrate concentrations approached seawater with a minimum observed nitrate concentration of 1.26 µmol NO_3^- L^{-1} and a maximum concentration of 2.17 µmol NO_3^- L^{-1} (Fig. 4g). During ebb tide, nitrate slightly increased by 0.92 µmol NO_3^- L^{-1} (ΔNO_3^-), resulting in a nitrate increase of 0.13 µmol NO_3^- L^{-1} h^{-1}.

Ammonium increased from 3.47 µmol NH_4^+ L^{-1} to 6.22 µmol NH_4^+ L^{-1} during ebb tide (Fig. 4h). We observed an ammonium increase (ΔNH_4^+) of 2.74 µmol NH_4^+ L^{-1} resulting in an increase of 0.4 µmol NH_4^+ L^{-1} h^{-1}.

C_{org}:N ratios of SPM increased during ebb tide (Fig. 4i). We observed a minimum C_{org}:N ratio of 5.6 around high tide that increased to a maximum of 13.0 during ebb tide. Simultaneously, the SPM concentration increased during ebb tide, from 12.8 mg L^{-1} to a maximum of 82.4 mg L^{-1} at the second last station (Table 1).

https://doi.org/10.5194/egusphere-2023-2595
Preprint. Discussion started: 9 November 2023

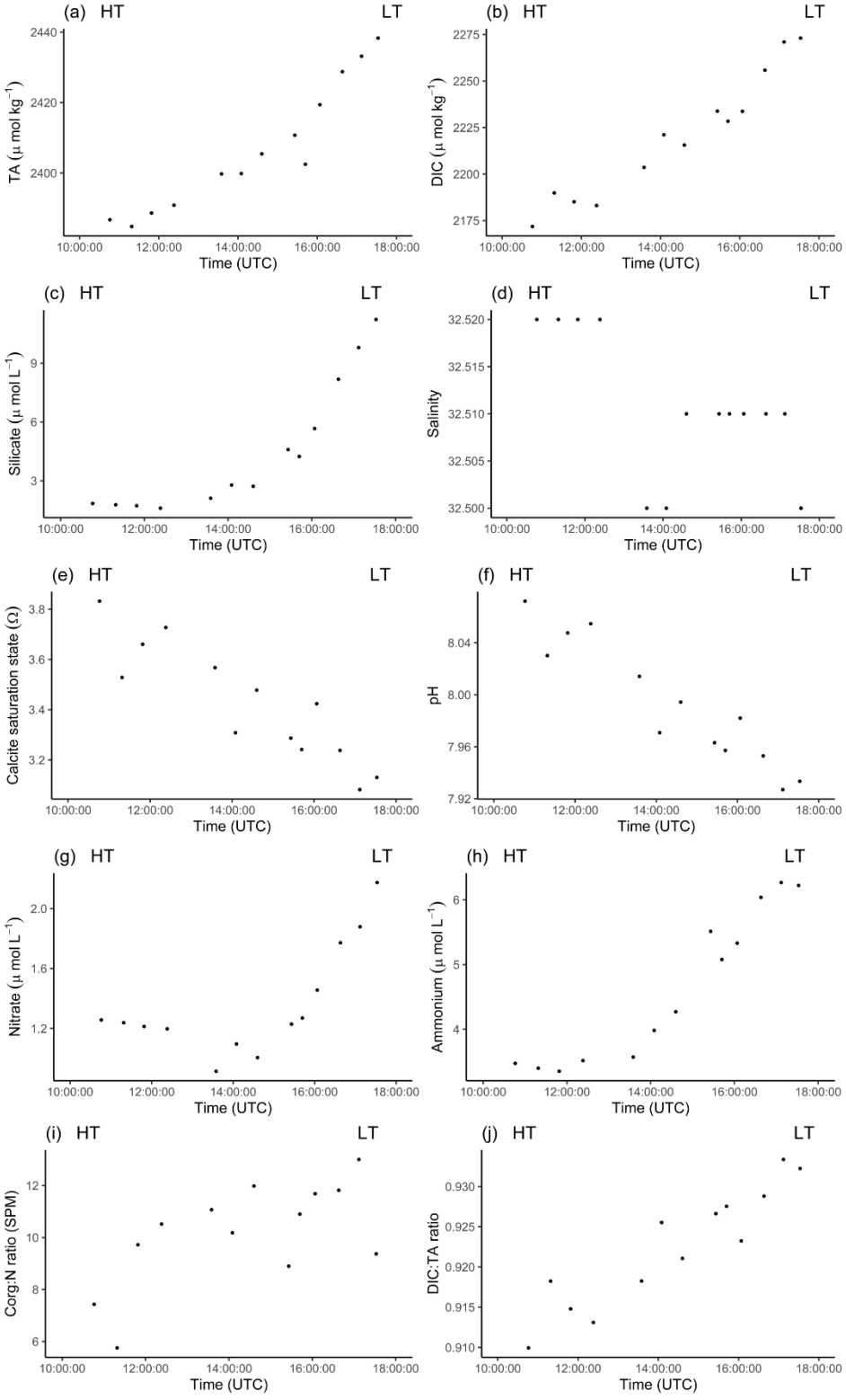

https://doi.org/10.5194/egusphere-2023-2595
Preprint. Discussion started: 9 November 2023

Figure 4 Tidal cycle. Temporal distribution of a) total alkalinity (TA), b) dissolved inorganic carbon (DIC), c) silicate, d) salinity, e) calcite saturation state (Ω), f) pH, g) nitrate, h) ammonium, i) C_{org}:N ratio of SPM from high tide to low tide. Note the different y-axes.

Table 1 Tidal cycle sample parameter during ebb tide. Sample no. 545 is the first sample at high tide and sample no. 557 is the last sample at ebb tide on May 21st 2019. Shown are rounded up values of the various parameters per sample.

Sample No.	Temp [°C]	Sal	TA [µmol kg^{-1}]	DIC [µmol kg^{-1}]	Si [µmol L^{-1}]	NO_3^- [µmol L^{-1}]	NO_2^- [µmol L^{-1}]	NH_4^+ [µmol L^{-1}]
545	13.26	32.52	2387	2172	1.84	1.26	0.19	3.47
546	13.25	32.52	2385	2190	1.77	1.24	0.19	3.40
547	13.28	32.52	2389	2185	1.72	1.21	0.19	3.35
548	13.38	32.52	2391	2183	1.6	1.19	0.19	3.52
549	14.32	32.50	2400	2204	2.11	0.91	0.25	3.57
550	14.61	32.50	2400	2221	2.78	1.09	0.29	3.98
551	14.64	32.51	2405	2216	2.72	1.01	0.29	4.27
552	14.73	32.51	2411	2234	4.59	1.23	0.34	5.51
553	14.77	32.51	2402	2228	4.24	1.26	0.33	5.08
554	14.72	32.51	2419	2234	5.66	1.46	0.36	5.33
555	14.66	32.51	2428	2256	8.18	1.77	0.43	6.04
556	14.68	32.51	2433	2271	9.79	1.87	0.47	6.27
557	14.70	32.50	2438	2273	11.22	2.17	0.50	6.22
Sample No.	DIN [µmol L^{-1}]	C / C_{org} (SPM) [µmol L^{-1}]	N (SPM) [µmol L^{-1}]	C_{org}:N (SPM)	SPM [mg L^{-1}]	Calcite [Ω]	pH	PO_4^{3-} [µmol L^{-1}]
545	4.93	86.8 / 65.1	8.8	7.4	12.8	3.8	8.07	0.12
546	4.83	72.7 / 42.4	7.4	5.8	8.7	3.5	8.03	0.11
547	4.76	112.4 / 93.4	9.6	9.7	15.4	3.7	8.05	0.11
548	4.91	108.5 / 104.6	9.9	10.5	16.8	3.7	8.05	0.12
549	4.73	111.1 / 97.8	8.8	11.1	13.9	3.6	8.01	0.32
550	5.37	233.0 / 180.3	17.7	10.2	32.2	3.3	7.97	0.42
551	5.56	193.2 / 174.3	14.5	12.0	29.6	3.5	7.99	0.47
552	7.08	248.6 / 163.5	18.4	8.9	34.3	3.3	7.96	0.57
553	6.67	257.6 / 199.3	18.3	10.9	41.6	3.2	7.95	0.54
554	7.15	324.4 / 271.1	23.2	11.7	55.0	3.4	7.98	0.54
555	8.24	440.4 / 345.2	29.2	11.8	75.7	3.2	7.95	0.58
556	8.61	430.5 / 363.3	27.9	13.0	82.4	3.1	7.93.	0.62
557	8.90	308.9 / 199.1	21.2	9.4	48.8	3.1	7.93	0.63

https://doi.org/10.5194/egusphere-2023-2595
Preprint. Discussion started: 9 November 2023

3.3 TA generation

The Dutch Wadden Sea is exposed to strong tidal forcing by the North Sea leading to a bi-diurnal exchange of water. The strong tidal forcing highlights the benthic-pelagic coupling and let us assume that the outflowing water exports material from the sediment. In order to support our assumption, we further investigated potential TA sources.

For a first rough estimate of a maximum TA export during ebb tide, we used the observed TA increase (ΔTA) of 51.6 µmol kg^{-1} during ebb tide observed at an anchor station in the Ameland Inlet, and the tidal prism of 478 $*10^6$ m^3 the Ameland Inlet (Louters and Gerritsen, 1994). With this estimate, we arrived at a rough TA export on the order of 23.9 mol TA during ebb tide from the Ameland Inlet into the North Sea. With an observed tidal duration of 6.8 h, the estimated TA export of 23.9 mol would result in a TA export of 3.5 mol h^{-1}.

For a further source location of the generated TA, we checked various correlations and relations.

Based on the correlation of TA and silicate, and the relation between both and salinity, we were able to determine whether TA originates in the Wadden Sea or is carried by river runoff. Both, TA and silicate increased almost proportionally during ebb tide, pointing to the same origin (Fig. 5b). The similar pattern of TA over salinity and silicate over salinity suggested non-conservative behavior of both, and rules out any sources due to fresh water dilution and river runoff (Table 1).

In order to further shed light on potential TA sources in the Dutch Wadden Sea, we correlated TA with various parameters during ebb tide, i.e., from high tide to low tide. Thereby, the first four samples on the left plot side of the plots in Fig. 5 show values probably at the tipping point of high tide and we recommend neglecting these samples in the interpretation of ebb tide samples. The observation of samples collected during ebb tide allowed us to examine potential sources of TA generation.

First, we tested the correlation between TA and DIC that reveals the ratio between anaerobic and aerobic processes. We identified a strong positive correlation between DIC and TA with TA concentrations > DIC concentrations (Fig. 5a). However, even when TA concentrations were higher than DIC concentrations, the slope of 1.77 indicated DIC release excess with an increase in DIC (ΔDIC = 101.3 µmol kg^{-1}) almost twice as high as TA (ΔTA = 51.6 µmol kg^{-1}) (Fig. 5a). This may be caused by strong CO_2 production due to high aerobic OM degradation, or uptake from the atmosphere by enhanced water movement. The TA increase can be fueled by various processes which we will discuss at later stage.

We detected an almost linear positive correlation of increasing TA and silicate during ebb tide, supporting the out washing process from the pore-water (Fig. 5b). We identified a stronger influence of the pore-water with ongoing ebb tide.

The positive correlation between nitrate and TA was lower than both previous correlations with a $R^2 = 0.67$ (Fig. 5c), which could be traced back on an effect of the first four samplings as mentioned above. In the remaining samples, we observed increasing nitrate and TA concentrations, suggesting a stronger effect of TA generation than nitrate production.

https://doi.org/10.5194/egusphere-2023-2595
Preprint. Discussion started: 9 November 2023

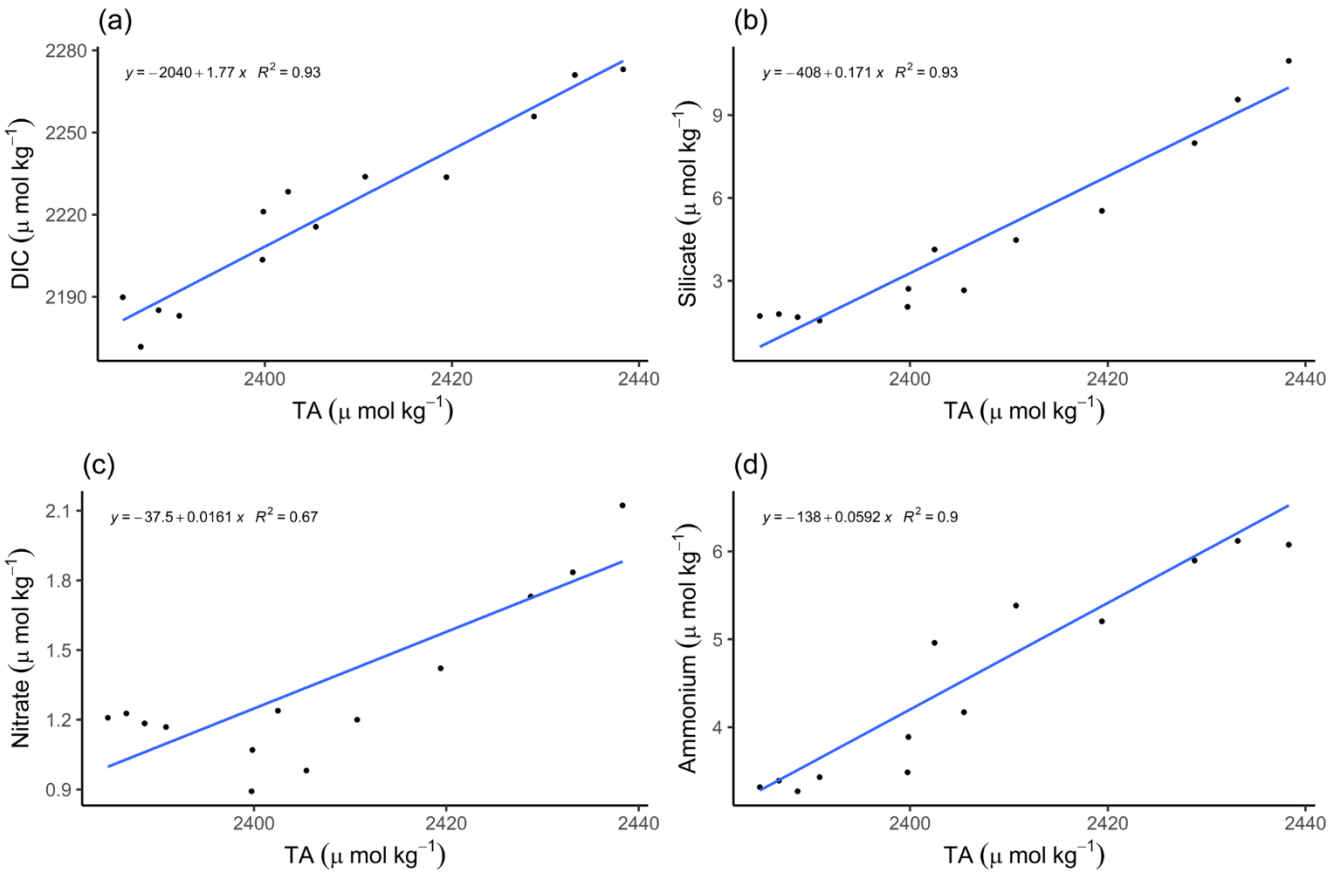

Figure 5 TA correlations. Correlations of TA with a) dissolved inorganic carbon (DIC), b) silicate, c) nitrate, and d) ammonium during ebb tide in the Ameland Inlet.

4 Discussion

4.1 Spatial TA variability

In the past, Hoppema (1990) reported TA distributions in the most western Wadden Sea around the barrier islands Texel, Vlieland, and Terschelling. He focused on the tidal basins drained by the tidal inlets Marsdiep and Vlie located more western than our sampling stations.

Hoppema (1990) did not observe an increase of salinity in the Wadden Sea from the fresh water source towards the ocean and associated this to the influence of tidal differences. In most parts of the Wadden Sea we also did not observe an increasing salinity with distance from the coast but a constant marine salinity. Increasing salinity with distance from the coast was only detected in the large Ems Estuary with high discharges of fresh water, and close to Harlingen and Lauwersoog, which directly have fresh water inflows by smaller rivers. Beside this, the Wadden Sea is clearly dominated by coastal North Sea water with

https://doi.org/10.5194/egusphere-2023-2595
Preprint. Discussion started: 9 November 2023

relatively high salinities. The occurrence of marine water in the entire Wadden Sea and on the tidal flats is supported by our transect data that revealed relatively high salinities at coastal North Sea level in the entire Wadden Sea.

While the spatial TA data by Hoppema (1990), showed lower TA concentrations at stations with more fresh water influence and higher TA concentrations in the tidal inlets, we observed high TA concentrations at stations with fresh water influence and lower TA concentrations in the tidal inlets. This result suggests TA generation in sediments, which is fueled by high imports of nutrients and OM (Van Beusekom and De Jonge, 2002). In May, Hoppema's (1990) data showed TA concentrations ranging between 2319 and 2444 µmol kg^{-1} at salinities between 18.62 and 29.17, while our lowest observed TA concentration was 2332 µmol kg^{-1} at a salinity of 32.14, and our highest TA concentration was 2517 µmol kg^{-1} at a salinity of 20.25. In addition to the spatial differences, the general level of TA was only slightly higher in our data than in the data from the early 1990s.

A conservative mixing between TA and salinity is only visible in the Ems-Dollard Inlet and the Vlie Inlet (Fig. 3). For the Vlie Inlet, this can be explained by the fact that more water masses from the North Sea pass through the deeper inlets and transport more seawater towards the coast. The Vlie Inlet is the one with the highest average tidal prism and the second largest inlet after the Marsdiep Inlet in the Dutch Wadden Sea (Elias et al., 2012). Similar to our findings, Hoppema (1990) noted a linear mixing of TA and salinity in the Vlie Inlet during his time, and suspected a lower fresh water content there as well.

For the Ems-Dollard Inlet, the Ems River discharges more fresh water and therefore dominates the mixing. In a previous study, Norbisrath et al. (2023) observed very high TA concentrations and TA generation in the tidal river of the highly turbid Ems Estuary, which may explain the high levels of TA in the estuary (at low salinities) that we observed in this study.

Compared to the past, our initial TA values in the Vlie Inlet sampled in May were somewhat higher than in Hoppema (1990), where he sampled in June and August. His TA values measured in the Marsdiep Inlet in May were in a similar range to ours, but the inlet is located more western with a higher impact from the North Sea and the IJsselmeer.

Hoppema (1990) also identified varying TA concentrations within the Dutch Wadden Sea and related these to different sinks and sources. TA sinks can be calcium carbonate ($CaCO_3$) precipitation, or extraction of seawater carbonate by mollusks (Chen and Wang, 1999;Hoppema, 1990). Variable fresh water inflows can either serve as a sink or a source (Chen and Wang, 1999;Hoppema, 1990). Other sources can be $CaCO_3$ dissolution, anaerobic metabolic processes in the sediment, or erosion of TA enhancing sediments (Hoppema, 1990;Chen and Wang, 1999).

Since we almost observed only marine salinities (> 30), and higher TA values in the Wadden Sea than in the North Sea, which is in contrast to Hoppema (1990), we exclude TA sinks and only focus on TA sources here. According to Hoppema (1990), the main causes for TA variations in the Dutch Wadden Sea were fresh water inflows and sources in the sediment. In our study, fresh water inflows with high TA concentrations were only observed in the Ems Estuary and Ems-Dollard Inlet. For a further TA source identification in the Dutch Wadden Sea, we observed the TA variability within a tidal cycle.

https://doi.org/10.5194/egusphere-2023-2595
Preprint. Discussion started: 9 November 2023

4.2 Determination of TA generation

Since Hoppema (1990) identified variations in the Wadden Sea's TA occurrence and distribution, and Burt et al. (2016) and Schwichtenberg et al. (2020) assumed TA generation in the Wadden Sea as an important source for the North Sea's carbon storage capacity, we want to further shed light on the TA generation and potential sources.

In a study from the early 1990s, Hoppema (1993) observed a tidal cycle in the Marsdiep in May and September, while he focused on TA, DIC, and oxygen. In his study, salinity values between 21 and 26, which were lower than ours (> 32), were observed. Hoppema (1993) also observed increasing TA values during ebb tide and assumed the tidal flats and discharging rivers and canals as sources of TA.

We detected no large differences between our data and the TA values during a tidal cycle observed by Hoppema (1993). However, an in-depth interpretation and comparison exceed the capacity of the data.

Since we observed a generation of 7.6 µmol TA kg^{-1} h^{-1} during ebb tide, we also support the assumption of the Wadden Sea being a TA source for the North Sea.

With the tidal prism of the Ameland Inlet by Louters and Gerritsen (1994), we estimated a first rough potential maximum TA export from the Wadden Sea into the North Sea on the order of 23.9 mol TA during ebb tide (3.5 mol h^{-1}) at least between spring and summer. This amount is just a maximum estimate, because some water in the main tide ways and channels have no direct contact to the areas of the tidal flats. Since we only have one value of one tidal observation, an inclusion into the model used by Schwichtenberg et al. (2020) would be unreliable (personal communication J. Pätsch, 2022). Schwichtenberg et al. (2020) assumed an export of 10 to 14 Gmol TA yr^{-1} for the entire Dutch Wadden Sea. Whether our TA generation would match their suggested TA export, more observational data are required. At least, observational data of each season are mandatory to run the model and gain a representative result (personal communication J. Pätsch, 2022), which we suggest as future work.

4.3 TA source attribution

4.3.1 Local sediment outwash

In order to gain further inside into potential sources of TA, we included nutrients in our investigation. The main focus was on silicate that we used as a natural tracer since it is not directly provided anthropogenically and allowed us to determine the silicate source (Van Der Zee and Chou, 2005). In the silicate concentrations, we identified a silicate increase of 1.4 µmol Si L^{-1} h^{-1} during ebb tide. Silicate originates from dissolution of diatoms and sediment outwash in the Wadden Sea (Van Bennekom et al., 1974;Van Der Zee and Chou, 2005).

Here, we relate the silicate increase to outwash from sediments, because it markedly increased during ebb tide. This assumption can be supported by Van Bennekom et al. (1974), who suggested silicate diffusion from interstitial water in the sediment as potential source, since very high silicate concentrations were found in deeper sediment layers (Rutgers van der Loeff, 1974). Due to the absence of large estuaries nearby and a salinity consistently above 32, we exclude fresh water runoff as a silicate

https://doi.org/10.5194/egusphere-2023-2595
Preprint. Discussion started: 9 November 2023

source here. This can be supported by the relation between silicate and salinity in which we observed a non-conservative behavior (Table 1). Since TA behave also non-conservative relative to salinity (Table 1), the occurrence of TA sources in the tidal flats of the Wadden Sea other than river runoff is supported.

Submarine groundwater discharge (SGD) was identified as a source for nutrient fluxes in tidal flat ecosystems in previous studies (e.g., Santos et al., 2021;Waska and Kim, 2011;Wu et al., 2013). Waska and Kim (2011) identified strong SGD contributing up to 50 to 70 % of the nutrient fluxes that fuel primary production in a tidal embayment (Hampyeong Bay) in southwest Korea. In May, they observed low salinities indicating fresh water. However, in September they observed constant marine salinities referring them to be exclusively composed of recirculating seawater. Since we only observed marine salinities here, we suspect that recirculating marine groundwater enriched with nutrients could also act as a source for our observed parameters.

TA generation in tidal flats was also observed by Faber et al. (2014), who focused on a large macro tidal embayment in southern Australia. They also found increasing TA values during ebb tide. Because they used ^{222}Rn (radon-222) as a conservative tracer to detect pore-water exchange, they were able to associate the TA increase with a higher fraction of pore-water, which contained higher TA concentrations, and determined the tidal cycle as the controlling force for pore-water exchange. With this explanation and the indicated silicate outwash, our assumption that TA is generated in the sediments of the tidal flats in the Dutch Wadden Sea and is washed out during ebb tide is supported. The increase in TA and silicate is clearly a tidal signal. In addition, since the observed marine TA concentrations in the Vlie Inlet, except of the two samples near Harlingen, were in the same range as the other observed TA concentrations and were below the increasing TA concentrations during ebb tide, we exclude lateral advected signals. We clearly identify TA generation here as local sources in the sediments of the tidal flats.

4.3.2 TA generating processes

The observed TA generation of 7.6 µmol TA kg^{-1} h^{-1} and the silicate increase of 1.4 µmol Si L^{-1} h^{-1} indicated an excess of TA under consideration of a TA:silicate ratio of 2:1 (Marx et al. 2017), and under the condition of silicate being bound in minerals, which would then account for a TA generation of 2.8 µmol TA kg^{-1} h^{-1}. However, when silicate occurred dissolved in water it does not contribute to TA generation (Meister et al., 2022). A TA excess related to silicate was also observed in the correlation between TA and silicate (Fig. 5b). Since we observed more TA generated than silicate being washed out, other biogeochemical processes must be responsible for the TA generation in the sediments of the tidal flats in the Dutch Wadden Sea.

With the observed omega values, we exclude $CaCO_3$ dissolution as TA source in the overlying water, since the omega values were clearly supersaturated with $\Omega > 1$(Fig. 4e). The continuous calcite supersaturation nicely indicated the inflow and dominance of North Sea water during the flood, with omega values similar to previously observed North Sea values ($\Omega \sim 3.5$ to 4) (Charalampopoulou et al., 2011;Carter et al., 2014). However, because of the Ω supersaturation of the overlying water and a lack of pore-water data, we were unable to determine if TA generation by $CaCO_3$ dissolution occurs in deeper sediment layers. There, $CaCO_3$ dissolution can only be driven metabolically, when CO_2 is produced during OM remineralization or

https://doi.org/10.5194/egusphere-2023-2595
Preprint. Discussion started: 9 November 2023

reduced compounds that were previously produced during anaerobic processes are oxidized and lead to undersaturation with respect to carbonates (Brenner et al., 2016;Jahnke et al., 1994).

By a more detailed interpretation of ΔDIC, ΔTA, and various nutrient ratios, we tried to further narrow down the potential sources of TA generation in the sediments and used an upper bound estimate for $CaCO_3$ dissolution.

The correlation of DIC and TA reveals an excess of released DIC compared to TA (Fig. 5a), as indicated by the slope of 1.77, while we observed an increase in DIC (ΔDIC) almost twice as high as in TA (ΔTA). The high ΔDIC points to high aerobic OM degradation and remineralization, resulting in high CO_2 export. High aerobic OM degradation was also previously observed in the Wadden Sea (e.g., De Beer et al., 2005), assuming an OM degradation and remineralization occurring in the water and sediment in about equal parts (Van Beusekom et al., 1999). High OM degradation is also indicated by the increasing C_{org}:N ratios of SPM during ebb tide (Table 1). Because we observed constant coastal North Sea salinities, we rule out fresh water runoff and terrestrial signals as source for the increasing C_{org}:N ratios of SPM. We assume that fresh OM is rapidly degraded, and the older OM settle on and in the sediment where the degradation continuous and where it is resuspended by the water exchange with outflowing water. Therefore, we assume that the increase of SPM concentrations and their C_{org}:N ratios is an indicator for older and more refractory OM.

The increase in TA concentrations point to anaerobic processes, $CaCO_3$ dissolution, or a combination thereof as TA source occurring in the sediments.

For the upper bound estimate, we assumed $CaCO_3$ dissolution in the sediments with the DIC:TA ratio of 1:2 as source of TA. Considering this ratio and the observed ΔTA of 51.6 µmol TA kg^{-1}, a potential ΔDIC of 25.8 µmol DIC kg^{-1} of the observed ΔTA would be produced by $CaCO_3$ dissolution. The remaining potential 75.5 µmol DIC kg^{-1} (101.3 – 25.8 µmol DIC kg^{-1}) of the observed (ΔDIC) could then be produced by OM degradation and remineralization, and would, using the expected Redfield ratio of C:N (6.6), correspond to an estimated potential dissolved inorganic nitrogen (DIN) production of 11.4 µmol kg^{-1}. This estimated potential DIN production (11.4 µmol kg^{-1}) of OM degradation and remineralization exceeded the observed increase of ΔDIN (3.97 µmol L^{-1}; Table 1, sum of NO_3^-, NO_2^- and NH_4^+) during ebb tide. With this estimation and the assumption that all DIN produced is released and thus lost, TA is probably produced by $CaCO_3$ dissolution and anaerobic metabolic processes other than denitrification in the sediment. In addition to that, and with a N-focused perspective, the DIN loss also hints to the occurrence of other processes that consume nitrogen species but have no net effect on TA, such as anammox and coupled nitrification-denitrification (Hu and Cai, 2011;Middelburg et al., 2020). The suggested DIN loss can be supported by considering the marine DIN:Si ratio, which is supposed to be 1:1 (Brzezinski, 1985). We observed DIN:Si ratios decreasing from 2.7 to 0.8 from high tide to low tide. The decreasing ratios show that both parameter concentrations increased during ebb tide, whereby DIN concentrations increased lower than silicate concentrations. We observed a silicate excess with respect to DIN at the end of ebb tide, supporting the DIN loss.

Denitrification, the anaerobic irreversible reduction of NO_3^- to N_2 that generates 0.9 mole TA by using 1 mole NO_3^- as electron acceptor (Chen and Wang, 1999) is a net TA source. Denitrification depends on the supply of nitrate, which seasonally varies (Van Der Zee and Chou, 2005 and references therein). Generally, nitrate is depleted in summer due to high turnover rates and

https://doi.org/10.5194/egusphere-2023-2595
Preprint. Discussion started: 9 November 2023

occurs in higher concentrations in winter (Kieskamp et al., 1991;Jensen et al., 1996;Van Der Zee and Chou, 2005). This seasonality lead to denitrification rates also being lower in summer and higher in winter (Kieskamp et al., 1991;Jensen et al., 1996). In previous studies, Faber et al. (2014) identified denitrification as a minor source for TA due to low denitrification rates, and also Kieskamp et al. (1991) observed low denitrification rates in the Wadden Sea, with low nitrate concentrations (< 2.5 µmol L^{-1}) in the overlying water. Because we observed nitrate concentrations (< 2.17 µmol L^{-1}) lower than the concentration sufficient for denitrification assumed by Kieskamp et al. (1991), we do not exclude denitrification, but suspect it as a minor source for TA in the Dutch Wadden Sea at least in spring and summer due to the seasonal lack of nitrate. Thomas et al. (2009) detected TA seasonality in the southern bight of the North Sea, which is also influenced by the TA generation in the Wadden Sea. We support their findings of lowered TA generation by denitrification in late spring and early summer. In addition, the calculated potential DIN excess compared to the observed DIN not only hints to other N consuming processes that have no effect on TA, but also suggests that allochthonous nitrate would be needed to fuel the TA increase by denitrification. In addition, the albeit low availability of nitrate indicates to predominantly aerobic metabolic activity during the time of our observations, which is in line with earlier studies reporting an enhanced relevance of anaerobic activity later in summer (Luff and Moll, 2004;Thomas et al., 2009).

Another source of TA in sediments is aerobic OM respiration with the associated formation of ammonium while consuming H^+ (Blackburn and Henriksen, 1983;Berner et al., 1970;Brenner et al., 2016). The observed increasing ammonium (Fig. 4g) could be associated with aerobic OM degradation resulting in ammonium formation, i.e., ammonium increase in the upper oxygenated sediment layers, which would increase DIC by the production of CO_2, and increase TA by the consumption of H^+ (Fig.5) (Brenner et al., 2016). In sediments, then the production of one mole ammonium (from ammonia) would generate one mole TA (Berner et al., 1970;Meister et al., 2022). In contrast, in the water column, the aerobic respiration of OM produce CO_2 and increase DIC, also visible in decreasing pH values (Fig. 4f), but consume TA and would not produce ammonium (Chen and Wang, 1999). Therefore, aerobic OM respiration in the water column could only explain the higher increase in DIC than in TA, but not the simultaneous increase in TA and ammonium (Fig. 5). Based on this, we assume that OM respiration associated with TA generation occurs in the sediment, leading to TA and DIC generation and also to ammonium production, which are then washed out during ebb tide. The produced ammonium is then also accessible for nitrification that produces nitrate. A slightly increased nitrate concentration in the most upper sediment layers was observed by Beck et al. (2008a) in the German Wadden Sea. This observation, a potential nitrate reservoir, nitrate production due to OM degradation and nitrification occurring in the upper oxygenated sediment layers (Martin and Sayles, 1996), or a mix thereof could explain the low increasing nitrate concentrations during ebb tide. However, as we rule out terrestrial nitrate imports as nitrate source here, the simultaneous increase of TA and nitrate is noticeable for us, because nitrification consumes TA (Brenner et al., 2016). Here, we assume that potential nitrification has a minor effect on TA, because we observed only low nitrate concentrations and a really low increase of nitrate compared to the increase of ammonium and TA during ebb tide. The low nitrate concentrations resulting in reduced availability of bound oxygen, i.e., electron acceptors, promote the occurrence of other anaerobic processes

https://doi.org/10.5194/egusphere-2023-2595
Preprint. Discussion started: 9 November 2023

of the redox system, such as sulfate and iron reduction, to generate TA in the deeper, anoxic sediment layers in the Dutch Wadden Sea.

Sulfate reduction followed by iron reduction and the formation and burial of pyrite are net sources of TA, since TA consumption by reoxidation is excluded when buried in sediments (Berner et al., 1970;Faber et al., 2014). Whether these processes contribute to TA generation in the deeper sediments of the Dutch Wadden Sea cannot be further identified without the necessary data. However, sulfate reduction was also mentioned as source of TA by Thomas et al. (2009). The temporary slight appearance of noticeable sulfuric odor could be another indirect indicator for the occurrence of sulfate reduction. In previous studies of tidal flats in the German Wadden Sea, Beck et al. (2008a);(2008b) observed increasing TA concentrations with depth and identified sulfate reduction as the most important process for anaerobic OM remineralization in pore-water cores. Sulfate reduction releases 1.14 mole TA with the oxidation of one mole carbon of POC , and iron reduction releases 8.14 mole TA with the oxidation of one mole carbon of POC, indicating that both processes are large sources of TA generation (Brenner et al., 2016), but cannot be further interpreted without the necessary data.

A strict comparison of the northern and the western parts of the Wadden Sea cannot be fully recommended because the areas vary in terms of OM import and eutrophication effects (Van Beusekom et al., 2019), sediment composition, and extent between the barrier islands and the mainland, all of which influence the occurrence and interaction of biogeochemical processes (Schwichtenberg et al., 2020). Although, the area characteristics of northern and western Wadden Sea differ, a previous study by Brasse et al. (1999) identified high TA and DIC concentrations in the sediment of the North Frisian Wadden Sea and identified $CaCO_3$ dissolution and sulfate reduction as major TA sources, which appear consistent with our findings.

5 Conclusion

The Dutch Wadden Sea is a unique and highly dynamic ecosystem. While observing the spatial TA distribution and TA generation in the Dutch Wadden Sea, we detected higher TA values than in the North Sea, and identified the Dutch Wadden Sea clearly as a TA source of the North Sea's carbonate system. Compared to the TA values of the previous studies by Hoppema (1990);(1993), the TA values we observed were in a similar range, but while he observed lower TA values near the coast, we found higher ones there. However, more data from various seasons would be needed for a better comparison between then and now, and for a more precise status of TA.

By observing salinity and using silicate as a tracer, we excluded fresh water dilution and river runoff as TA sources and instead identified outwash from tidal flat sediments as sources of TA. Aerobic, metabolic processes such as $CaCO_3$ dissolution and ammonium formation seem to dominate TA generation in the upper oxic sediment layers and the overlying water, while anaerobic, metabolic processes such as denitrification, sulfate and iron reduction are potential TA sources in the deeper anoxic sediment layers. However, in spring and early summer, denitrification seems to play a minor role in generating TA in the sediments of the Dutch Wadden Sea due to seasonality and associated limited nitrate availability.

https://doi.org/10.5194/egusphere-2023-2595
Preprint. Discussion started: 9 November 2023

Data availability

The data of this study are either presented in the article or are available upon request from the corresponding author.

Author Contributions

MN wrote the manuscript, did the carbon sampling and sample measurement, analyzed and evaluated the data, and led the study. JvB led the research cruise. JvB and HT contributed with editorial and scientific recommendations. MN prepared the manuscript with contribution from all co-authors.

Competing interests

The contact author has declared that none of the authors has any competing interests.

Acknowledgement

We thank the crew from RV *Ludwig Prandtl* for their support during the cruise. We thank Leon Schmidt for the nutrient sampling and measurements.

Financial support

This research has been funded by the German Academic Exchange Service (DAAD, project: MOPGA-GRI, grant no. 57429828), which received funds from the German Federal Ministry of Education and Research (BMBF).

References

Abril, G., and Frankignoulle, M.: Nitrogen–alkalinity interactions in the highly polluted Scheldt basin (Belgium), Water Research, 35, 844-850, 2001.

Beck, M., Dellwig, O., Holstein, J. M., Grunwald, M., Liebezeit, G., Schnetger, B., and Brumsack, H.-J.: Sulphate, dissolved organic carbon, nutrients and terminal metabolic products in deep pore waters of an intertidal flat, Biogeochemistry, 89, 221-238, 2008a.

Beck, M., Dellwig, O., Liebezeit, G., Schnetger, B., and Brumsack, H.-J.: Spatial and seasonal variations of sulphate, dissolved organic carbon, and nutrients in deep pore waters of intertidal flat sediments, Estuarine, Coastal and Shelf Science, 79, 307-316, 2008b.

Berner, R. A., Scott, M. R., and Thomlinson, C.: CARBONATE ALKALINITY IN THE PORE WATERS OF ANOXIC MARINE SEDIMENTS 1, Limnology and Oceanography, 15, 544-549, 1970.

Berner, R. A., Lasaga, A. C., and Garrels, R. M.: Carbonate-silicate geochemical cycle and its effect on atmospheric carbon dioxide over the past 100 million years, Am. J. Sci.;(United States), 283, doi:10.2475/ajs.283.7.641., 1983.

Blackburn, T., and Henriksen, K.: Nitrogen cycling in different types of sediments from Danish waters 1, Limnology and Oceanography, 28, 477-493, 1983.

Borges, A. V., Delille, B., and Frankignoulle, M.: Budgeting sinks and sources of CO2 in the coastal ocean: Diversity of ecosystems counts, Geophysical research letters, 32, doi.org/10.1029/2005GL023053, 2005.

Bozec, Y., Thomas, H., Elkalay, K., and de Baar, H. J.: The continental shelf pump for CO2 in the North Sea—evidence from summer observation, Marine Chemistry, 93, 131-147, 2005.

https://doi.org/10.5194/egusphere-2023-2595
Preprint. Discussion started: 9 November 2023

Brasse, S., Reimer, A., Seifert, R., and Michaelis, W.: The influence of intertidal mudflats on the dissolved inorganic carbon and total alkalinity distribution in the German Bight, southeastern North Sea, Journal of Sea Research, 42, 93-103, 1999.

Brenner, H., Braeckman, U., Le Guitton, M., and Meysman, F. J.: The impact of sedimentary alkalinity release on the water column CO2 system in the North Sea, Biogeosciences, 13, 841-863, 2016.

Brewer, P. G., and Goldman, J. C.: Alkalinity changes generated by phytoplankton growth 1, Limnology and Oceanography, 21, 108-117, 1976.

Brzezinski, M. A.: The Si: C: N ratio of marine diatoms: interspecific variability and the effect of some environmental variables 1, Journal of Phycology, 21, 347-357, 1985.

Burt, W., Thomas, H., Hagens, M., Pätsch, J., Clargo, N., Salt, L., Winde, V., and Böttcher, M.: Carbon sources in the North Sea evaluated by means of radium and stable carbon isotope tracers, Limnology and Oceanography, 61, 666-683, 2016.

Carter, B. R., Toggweiler, J., Key, R. M., and Sarmiento, J. L.: Processes determining the marine alkalinity and calcium carbonate saturation state distributions, Biogeosciences, 11, 7349-7362, 2014.

Charalampopoulou, A., Poulton, A. J., Tyrrell, T., and Lucas, M. I.: Irradiance and pH affect coccolithophore community composition on a transect between the North Sea and the Arctic Ocean, Marine Ecology Progress Series, 431, 25-43, 2011.

Chen, C. T. A., and Wang, S. L.: Carbon, alkalinity and nutrient budgets on the East China Sea continental shelf, Journal of Geophysical Research: Oceans, 104, 20675-20686, 1999.

Crutzen, P.: Geology of mankind, Nature, 415, https://doi.org/10.1038/415023a, 2002.

De Beer, D., Wenzhöfer, F., Ferdelman, T. G., Boehme, S. E., Huettel, M., van Beusekom, J. E., Böttcher, M. E., Musat, N., and Dubilier, N.: Transport and mineralization rates in North Sea sandy intertidal sediments, Sylt-Rømø basin, Wadden Sea, Limnology and Oceanography, 50, 113-127, 2005.

De Jonge, V., Essink, K., and Boddeke, R.: The Dutch Wadden Sea: a changed ecosystem, Hydrobiologia, 265, 45-71, 1993.

Dickson, A., and Millero, F. J.: A comparison of the equilibrium constants for the dissociation of carbonic acid in seawater media, Deep Sea Research Part A. Oceanographic Research Papers, 34, 1733-1743, 1987.

Dickson, A. G.: An exact definition of total alkalinity and a procedure for the estimation of alkalinity and total inorganic carbon from titration data, Deep Sea Research Part A. Oceanographic Research Papers, 28, 609-623, 1981.

Elias, E. P., Van der Spek, A. J., Wang, Z. B., and De Ronde, J.: Morphodynamic development and sediment budget of the Dutch Wadden Sea over the last century, Netherlands Journal of Geosciences, 91, 293-310, 2012.

Faber, P. A., Evrard, V., Woodland, R. J., Cartwright, I. C., and Cook, P. L.: Pore-water exchange driven by tidal pumping causes alkalinity export in two intertidal inlets, Limnology and Oceanography, 59, 1749-1763, 2014.

Glavovic, B., Limburg, K., Liu, K., Emeis, K., Thomas, H., Kremer, H., Avril, B., Zhang, J., Mulholland, M., and Glaser, M.: Living on the Margin in the Anthropocene: engagement arenas for sustainability research and action at the ocean–land interface, Current Opinion in Environmental Sustainability, 14, 232-238, 2015.

Grasshoff, K., Kremling, K., and Ehrhardt, M.: Methods of seawater analysis, John Wiley & Sons, 2009.

Hansen, H., and Koroleff, F.: Determination of nutrients. Methods of Seawater Analysis: Third, Completely Revised and Extended Edition. Grasshoff, K., Kremling, K., and Ehrhardt, M. (Eds.), Weinheim, Germany: Wiley-VCH Verlag GmbH, 2007.

Hoppema, J.: The distribution and seasonal variation of alkalinity in the southern bight of the North Sea and in the western Wadden Sea, Netherlands journal of sea research, 26, 11-23, 1990.

Hoppema, J.: The oxygen budget of the western Wadden Sea, The Netherlands, Estuarine, Coastal and Shelf Science, 32, 483-502, 1991.

Hoppema, J.: Carbon dioxide and oxygen disequilibrium in a tidal basin (Dutch Wadden Sea), Netherlands journal of sea research, 31, 221-229, 1993.

Hu, X., and Cai, W. J.: An assessment of ocean margin anaerobic processes on oceanic alkalinity budget, Global Biogeochemical Cycles, 25, doi.org/10.1029/2010GB003859, 2011.

Jahnke, R. A., Craven, D. B., and Gaillard, J.-F.: The influence of organic matter diagenesis on CaCO3 dissolution at the deep-sea floor, Geochimica et Cosmochimica Acta, 58, 2799-2809, 1994.

Jensen, K., Jensen, M., and Kristensen, E.: Nitrification and denitrification in Wadden Sea sediments (Königshafen, Island of Sylt, Germany) as measured by nitrogen isotope pairing and isotope dilution, Aquatic Microbial Ecology, 11, 181-191, 1996.

Keith, D. W., Ha-Duong, M., and Stolaroff, J. K.: Climate strategy with CO2 capture from the air, Climatic Change, 74, 17-45, 2006.

Kérouel, R., and Aminot, A.: Fluorometric determination of ammonia in sea and estuarine waters by direct segmented flow analysis, Marine Chemistry, 57, 265-275, 1997.

Kieskamp, W. M., Lohse, L., Epping, E., and Helder, W.: Seasonal variation in denitrification rates and nitrous oxide fluxes in intertidal sediments of the western Wadden Sea, Marine ecology progress series. Oldendorf, 72, 145-151, 1991.

Lewis, E., and Wallace, D.: Program developed for CO2 system calculations, Environmental System Science Data Infrastructure for a Virtual Ecosystem, 1998.

Louters, T., and Gerritsen, F.: The Riddle of the Sands: A Tidal SystenVs Answer to a Rising Sea Level, report RIKZ-94.040 (isbn 90-369-0084-0), 1994.

https://doi.org/10.5194/egusphere-2023-2595
Preprint. Discussion started: 9 November 2023

Luff, R., and Moll, A.: Seasonal dynamics of the North Sea sediments using a three-dimensional coupled sediment–water model system, Continental Shelf Research, 24, 1099-1127, 2004.
Martin, W., and Sayles, F.: CaCO3 dissolution in sediments of the Ceara Rise, western equatorial Atlantic, Geochimica et Cosmochimica Acta, 60, 243-263, 1996.
Matthews, H. D., and Caldeira, K.: Stabilizing climate requires near-zero emissions, Geophysical research letters, 35, 2008.
Mehrbach, C., Culberson, C., Hawley, J., and Pytkowicx, R.: Measurement of the apparent dissociation constants of carbonic acid in seawater at atmospheric pressure 1, Limnology and oceanography, 18, 897-907, 1973.
Meister, P., Herda, G., Petrishcheva, E., Gier, S., Dickens, G. R., Bauer, C., and Liu, B.: Microbial Alkalinity Production and Silicate Alteration in Methane Charged Marine Sediments: Implications for Porewater Chemistry and Diagenetic Carbonate Formation, Geochemical Signals in Dynamic Sedimentary Systems Along Continental Margins, 2022.
Meybeck, M.: Global chemical weathering of surficial rocks estimated from river dissolved loads, American journal of science, 287, 401-428, 1987.
Middelburg, J. J., Soetaert, K., and Hagens, M.: Ocean alkalinity, buffering and biogeochemical processes, Reviews of Geophysics, 58, e2019RG000681, 2020.
Norbisrath, M., Pätsch, J., Dähnke, K., Sanders, T., Schulz, G., van Beusekom, J. E., and Thomas, H.: Metabolic alkalinity release from large port facilities (Hamburg, Germany) and impact on coastal carbon storage, Biogeosciences, 19, 5151-5165, 2022.
Norbisrath, M., Neumann, A., Dähnke, K., Sanders, T., Schöl, A., van Beusekom, J. E., and Thomas, H.: Alkalinity and nitrate dynamics reveal dominance of anammox in a hyper-turbid estuary, Biogeosciences, 20, 4307–4321, https://doi.org/10.5194/bg-20-4307-2023, 2023.
Petersen, W., Schroeder, F., and Bockelmann, F.-D.: FerryBox-Application of continuous water quality observations along transects in the North Sea, Ocean Dynamics, 61, 1541-1554, 2011.
Postma, H.: Hydrography of the Dutch Wadden sea, Arch. Neerl. Zool, 10, 405-511, 1954.
Raaphorst, W. v., and Veer, H. W.: The phosphorus budget of the Marsdiep tidal basin (Dutch Wadden Sea) in the period 1950–1985: importance of the exchange with the North Sea, in: North Sea—Estuaries Interactions, Springer, 21-38, 1990.
Renforth, P., and Henderson, G.: Assessing ocean alkalinity for carbon sequestration, Reviews of Geophysics, 55, 636-674, 2017.
Ridderinkhof, H., Zimmerman, J., and Philippart, M.: Tidal exchange between the North Sea and Dutch Wadden Sea and mixing time scales of the tidal basins, Netherlands Journal of Sea Research, 25, 331-350, 1990.
Rutgers van der Loeff, M.: Transport van reactief silikaat uit Waddenzee sediment naar het bovenstaande water, NIOZ-rapport, 1974.
Sabine, C. L., Feely, R. A., Gruber, N., Key, R. M., Lee, K., Bullister, J. L., Wanninkhof, R., Wong, C., Wallace, D. W., and Tilbrook, B.: The oceanic sink for anthropogenic CO2, science, 305, 367-371, 2004.
Santos, I. R., Chen, X., Lecher, A. L., Sawyer, A. H., Moosdorf, N., Rodellas, V., Tamborski, J., Cho, H.-M., Dimova, N., and Sugimoto, R.: Submarine groundwater discharge impacts on coastal nutrient biogeochemistry, Nature Reviews Earth & Environment, 2, 307-323, 2021.
Schwichtenberg, F., Callies, U., and van Beusekom, J. E.: Residence times in shallow waters help explain regional differences in Wadden Sea eutrophication, Geo-Marine Letters, 37, 171-177, 2017.
Schwichtenberg, F., Pätsch, J., Böttcher, M. E., Thomas, H., Winde, V., and Emeis, K.-C.: The impact of intertidal areas on the carbonate system of the southern North Sea, Biogeosciences, 17, 4223-4245, 2020.
Shadwick, E., Thomas, H., Gratton, Y., Leong, D., Moore, S., Papakyriakou, T., and Prowe, A.: Export of Pacific carbon through the Arctic Archipelago to the North Atlantic, Continental Shelf Research, 31, 806-816, 2011.
Suchet, P. A., and Probst, J.-L.: Modelling of atmospheric CO2 consumption by chemical weathering of rocks: application to the Garonne, Congo and Amazon basins, Chemical Geology, 107, 205-210, 1993.
Thomas, H., Bozec, Y., Elkalay, K., and De Baar, H. J.: Enhanced open ocean storage of CO2 from shelf sea pumping, Science, 304, 1005-1008, 2004.
Thomas, H., Schiettecatte, L.-S., Suykens, K., Koné, Y., Shadwick, E., Prowe, A. F., Bozec, Y., de Baar, H. J., and Borges, A.: Enhanced ocean carbon storage from anaerobic alkalinity generation in coastal sediments, Biogeosciences, 6, 267-274, 2009.
Van Bennekom, A., Krijgsman-van Hartingsveld, E., Van der Veer, G., and Van Voorst, H.: The seasonal cycles of reactive silicate and suspended diatoms in the Dutch Wadden Sea, Netherlands Journal of Sea Research, 8, 174-207, 1974.
Van Beusekom, J., Brockmann, U., Hesse, K.-J., Hickel, W., Poremba, K., and Tillmann, U.: The importance of sediments in the transformation and turnover of nutrients and organic matter in the Wadden Sea and German Bight, Deutsche Hydrografische Zeitschrift, 51, 245-266, 1999.
Van Beusekom, J., and De Jonge, V.: Long-term changes in Wadden Sea nutrient cycles: importance of organic matter import from the North Sea, in: Nutrients and Eutrophication in Estuaries and Coastal Waters, Springer, 185-194, 2002.
Van Beusekom, J. E., Buschbaum, C., and Reise, K.: Wadden Sea tidal basins and the mediating role of the North Sea in ecological processes: scaling up of management?, Ocean & coastal management, 68, 69-78, 2012.
Van Beusekom, J. E., Carstensen, J., Dolch, T., Grage, A., Hofmeister, R., Lenhart, H., Kerimoglu, O., Kolbe, K., Pätsch, J., and Rick, J.: Wadden Sea Eutrophication: long-term trends and regional differences, Frontiers in Marine Science, 6, 370, doi.org/10.3389/fmars.2019.00370, 2019.
Van Der Zee, C., and Chou, L.: Seasonal cycling of phosphorus in the Southern Bight of the North Sea, Biogeosciences, 2, 27-42, 2005.

https://doi.org/10.5194/egusphere-2023-2595
Preprint. Discussion started: 9 November 2023

Waska, H., and Kim, G.: Submarine groundwater discharge (SGD) as a main nutrient source for benthic and water-column primary production in a large intertidal environment of the Yellow Sea, Journal of Sea Research, 65, 103-113, 2011.
Wolf-Gladrow, D. A., Zeebe, R. E., Klaas, C., Körtzinger, A., and Dickson, A. G.: Total alkalinity: The explicit conservative expression and its application to biogeochemical processes, Marine Chemistry, 106, 287-300, 2007.
Wu, Z., Zhou, H., Zhang, S., and Liu, Y.: Using 222Rn to estimate submarine groundwater discharge (SGD) and the associated nutrient fluxes into Xiangshan Bay, East China Sea, Marine pollution bulletin, 73, 183-191, 2013.
Zalasiewicz, J., Williams, M., Steffen, W., and Crutzen, P.: The new world of the Anthropocene. ACS Publications, 2010.
Zhang, C., Shi, T., Liu, J., He, Z., Thomas, H., Dong, H., Rinkevich, B., Wang, Y., Hyun, J.-H., and Weinbauer, M.: Eco-engineering approaches for ocean negative carbon emission, Science Bulletin, 2022.